Available online at www.sciencedirect.com
SCIENCE DIRECT
Catalysis Today 111 (2006) 74–83
CATALYSIS TODAY
www.elsevier.com/locate/cattod

Ultra-deep desulfurization and denitrogenation of diesel fuel by selective adsorption over three different adsorbents: A study on adsorptive selectivity and mechanism

Jae Hyung Kim, Xiaoliang Ma, Anning Zhou, Chunshan Song *

Clean Fuels and Catalysis Program, The Energy Institute and Department of Energy and Geo-Environmental Engineering, The Pennsylvania State University, 209 Academic Projects Building, University Park, PA 16802, USA

Available online 28 November 2005

Abstract

Adsorptive desulfurization and denitrogenation were studied using a model diesel fuel, which contains sulfur, nitrogen and aromatic compounds, over three typical adsorbents (activated carbon, activated alumina and nickel-based adsorbent) in a fixed-bed adsorption system. The adsorptive capacity and selectivity for the various compounds were examined and compared on the basis of the breakthrough curves. The electronic properties of the adsorbates were calculated by a semi-empirical quantum chemical method and compared with their adsorption selectivity. Different adsorptive selectivities in correlation with the electronic properties of the compounds provided new insight into the fundamental understanding of the adsorption mechanism over different adsorbents. For the supported nickel adsorbent, the direct interaction between the heteroatom in the adsorbates and the surface nickel plays an important role. The adsorption selectivity on the activated alumina depends dominantly on the molecular electrostatic potential and the acidic–basic interaction. The activated carbon shows higher adsorptive capacity and selectivity for both sulfur and nitrogen compounds, especially for the sulfur compounds with methyl substituents, such as 4,6-methyldibenzothiophene. Hydrogen bond interaction might play an important role in adsorptive desulfurization and denitrogenation over the activated carbon. Different adsorbents may be suitable for separating different sulfur compounds from different hydrocarbon streams.

Keywords: Adsorption; Desulfurization; Denitrogenation; Diesel fuel; Selectivity; Mechanism

1. Introduction

Due to the increasingly stringent environmental regulations on sulfur concentration in transportation fuels, ultra-deep desulfurization of diesel fuel has become a more and more important research subject [1–11]. This is because the sulfur compounds in the fuel are converted to SO_x during combustion, which not only results in acid rain, but also poisons catalysts in catalytic converters for reducing CO and NO_x [7–11]. Consequently, the sulfur level in diesel fuel must be reduced from current maximum 500 to 15 ppmw by 2006 in the US, and to 10 ppmw by 2010 in the EU. Further lower sulfur limit is expected for highway diesel fuels and also for nonroad diesel fuels in the near future. On the other hand, diesel fuel is also considered to be one of the promising liquid hydrocarbon fuels for producing H_2 for use in automotive and portable fuel cells due to its high energy density [1,2,7,8]. However, the sulfur compounds in the fuel and H_2S produced from them within hydrocarbon reforming process are poisons to reforming and shift catalysts as well as the electrode catalysts. Thus, sulfur concentration in the fuel needs to be reduced to less than 1 ppmw for proton exchange membrane fuel cell (PEMFC) and less than 10 ppmw for solid oxide fuel cell (SOFC) [1,2,7,8].

Hydrodesulfurization (HDS) at high temperature (320–380 °C) and high pressure (3–7 MPa) over CoMo or NiMo catalysts is currently a major process in petroleum refineries to reduce the sulfur in diesel fuel. Substantial advances have been achieved in new catalyst developments and new reactor technologies along with improved processes for producing low-sulfur gasoline and diesel fuels [1–11]. The major sulfur compounds existing in current commercial diesel are the alkyl dibenzothiophenes (DBTs) with one or two alkyl groups at 4- or/and 6-positions, which have been considered to be the refractory sulfur compounds in the fuel due to the steric hindrance of the

* Corresponding author. Tel.: +1 814 863 4466; fax: +1 814 865 3248.
E-mail address: csong@psu.edu (C. Song).

0920-5861/$ – see front matter © 2005 Elsevier B.V. All rights reserved.
doi:10.1016/j.cattod.2005.10.017

alkyl groups in HDS [7–12]. Consequently, it is difficult or very costly to use the existing HDS technology to reduce the sulfur in diesel fuel to less than 10 ppmw [3–8,12]. On the other hand, it has been observed that the nitrogen compounds coexisting in middle-distillate oil inhibit the ultra-deep HDS and the removal of such nitrogen compounds from the middle-distillate oil can improve significantly the ultra-deep HDS performance [13–17]. In addition, nitrogen compounds in the fuel and NH_3 produced from them during hydrocarbon reforming process are also poisons to the catalysts in hydrocarbon process and fuel cells, although the nitrogen concentration in diesel fuel is usually much lower than the sulfur concentration. In order to meet the need of ultra-clean diesel fuel for environmental protection and H_2 production, it is necessary to develop new approaches to ultra-deep desulfurization and denitrogenation.

Using adsorbents to selectively remove the sulfur and/or nitrogen compounds in liquid hydrocarbon fuels is one of the promising approaches for producing ultra clean fuels that not only meets the most stringent fuel specifications for transportation fuels, but also can be used for fuel cell applications. For the refinery applications, one potential new option is to use a sulfur-selective adsorption unit for ultra-deep removal of organic sulfur following a conventional HDS unit, and such a combination could remove all of the sulfur from the liquid fuel products.

As the diesel fuel contains not only sulfur compounds and nitrogen compounds but also a large number of aromatic compounds that have aromatic skeleton structure similar to the coexisting sulfur compounds, a great challenge in development of an effective adsorptive desulfurization process is to develop an adsorbent which can selectively adsorb the sulfur compounds. Recently, many attempts have been made to develop adsorbents for desulfurization of liquid hydrocarbon fuels [1,2,7,8]. The reported adsorbents include the reduced metals [18–24], metal oxides [25,26], metal sulfides [27], zeolite-based materials [28–32] and carbon materials [33–36]. In our previous studies [23,24], we found that the nickel-based adsorbents were good for removal of sulfur from commercial gasoline and jet fuel, while these types of adsorbents were not so successful for removing sulfur from the commercial diesel fuel. This is probably because the adsorption mechanism of the nickel-based adsorbents is based on a direct interaction between sulfur in the sulfur compounds and the active site on the adsorbent surface, and the alkyl groups at the 4- or/and 6-positions of DBTs inhibit the approach of the sulfur atom to the active sites.

Activated alumina has been used in chromatographic analysis and separation, and adsorptive separation. Recently, the use of activated alumina as an adsorbent in a desulfurization process for low-sulfur gasoline has been reported by Black & Veatch Irritchard Inc. and Alcoa Industrial Chemicals [37,38]. Activated carbon materials as porous materials with very high surface areas and large pore volume have been widely used in deodorization, decolorization, purification of drinking water, treatment of waste water, adsorption and separation of various organic and inorganic chemicals. Haji and Erkey reported using carbon aerogels as adsorbents for desulfurization of a model diesel (DBT in *n*-hexadecane) [33]. They found that the saturation adsorptive capacity of a carbon areogel with pore size of 22 nm was 15 mg of sulfur per gram of adsorbent (mg-S/g-A) and the carbon areogel selectively adsorbed DBT over naphthalene. Mochida and co-workers reported an interesting work on adsorptive desulfurization of real gas oil over activated carbon materials with surface area from 683 to 2972 m^2/g [34,35]. They found that using the activated carbon materials can remove sulfur and nitrogen species from gas oil. Recently, Hernandez-Maldonado et al. reported that using the activated carbon or activated alumina as adsorbent in a guard bed can improve the adsorptive performance of Cu(I)–Y zeolites [29,30]. However, many reported studies were based on the adsorptive desulfurization of real fuels and the absence of analytic data for the coexisting aromatics and nitrogen compounds, which makes it difficult to quantitatively analyze and compare the adsorptive selectivity of different adsorbents for various aromatic, sulfur and nitrogen compounds existing in the fuels, and to clarify the adsorption mechanism. The adsorptive mechanism and selectivity over various adsorbents are still unclear. In order to develop new adsorbents with high selectivity and high capacity, to modify the commercially available adsorbents, or to design a layered adsorbent bed for a practical application in ultra-deep desulfurization, it is critical to fundamentally understand the adsorptive mechanism and selectivity for various species over different adsorbents.

In the present study, adsorptive desulfurization and denitrogenation of a model diesel fuel, which contained the same molar concentration of the species examined, including sulfur compounds, nitrogen compounds and two-ring aromatic compounds, over three typical adsorbents, supported nickel, activated alumina and activated carbon, was conducted in a fixed-bed adsorption system at ambient temperature and atmospheric pressure. The adsorptive capacity and selectivity of the three adsorbents for the various species were examined and compared on the basis of the breakthrough curves. The electronic properties of the various species were calculated by a semi-empirical quantum chemical method and correlated with their adsorptive performance. The adsorptive selectivity and mechanism are discussed in combination of the experimental results and the quantum chemical calculations.

2. Experimental

In order to compare the adsorptive selectivity for aromatic, sulfur and nitrogen compounds in diesel, a model diesel fuel, which contained the same molar concentration of naphthalene (Nap), 1-methylnaphthalene (1-MNap), dibenzothiophene (DBT), 4,6-dimethyl-dibenzothiophene (4,6-DMDBT), indole and quinoline in a mixture solvent was prepared. The detailed composition of the model fuel is listed in Table 1. The molar concentration of each compound in the model fuel was 10.7 μmol/g. The corresponding total sulfur concentration and nitrogen concentration in the fuel was 687 and 303 ppmw, respectively. The model fuel also contained about 10 wt.% of butybenzene to mimic the monoaromatics in real diesel. All these compounds were purchased from Aldrich Chemical Co. and used as such without further purification.

Table 1
The concentration of each compound in model fuel

Chemicals	Concentration		Molar concentration (μmol/g)
	wt.%	ppmw S or N	
Sulfur compounds			
DBT (>99%)	0.20	343.3	10.7
4,6-DMDBT (>97%)	0.23	343.4	10.7
Total		686.7	
Nitrogen compounds			
Quinoline	0.14	152.0	10.8
Indole	0.13	151.0	10.8
Total		303.0	
Aromatics			
Naphthalene	0.14		10.7
1-Methylnaphthalene	0.16		10.7
tert-Butylbenzene	9.92		
Total	10.21		
Paraffins			
n-Decane	44.01		
n-Hexadecane (>99%)	44.02		
n-Tetradecane (>99%)	0.06	(Internal standard)	
Total	100.00		

The activated carbon was a commercial product, Nuchar SA 20, provided by Westvaco, which had surface area of 1843 m^2/g and average pore size of 28.6 Å. The acidic activated alumina employed as an adsorbent in the present study was purchased from Aldrich Chemical Co. It has a gamma crystalline phase with a surface area of 155 m^2/g and average pore size of 58 Å. The supported nickel (Ni/SiO_2-Al_2O_3) used in the present study contained about 55 wt.% of Ni in metallic state with silica-alumina as a support. It was prepared by the wet impregnation method and had a BET surface area of 157 m^2/g [39]. Before using, Ni/SiO_2-Al_2O_3 were pre-reduced in a flowing reactor under a H_2 flow at 500 °C for 5–6 h, and then, passivated using sulfur-free *n*-hexane and stored in the same solvent in an airtight sample bottle. Some properties of these three adsorbents are listed in Table 2.

Adsorptive desulfurization and denitrogenation of the model fuel over the three adsorbents was performed at ambient temperature, 25 °C. The pre-reduced Ni/SiO_2-Al_2O_3 was packed in a stainless steel column having a bed dimension of 4.6 mm i.d. and 150 mm length. The packed column was placed in a convection oven designed in our laboratory for the adsorption experiments. Before introducing the fuel into the adsorbent bed, the adsorbent bed was treated further with H_2 gas at a flow rate of 100 ml/min, heated up to 200 °C and kept at this temperature for about 1 h to remove hexane in the adsorbent. After the pretreatment, the temperature of the adsorbent bed was reduced to 25 °C for the subsequent adsorption experiments. For adsorption on the activated alumina and the activated carbon, the adsorbent was packed into the column, and pretreated under a nitrogen flow at 200 °C for 1 h in order to remove the adsorbed moisture and others, which might influence adsorptive performance significantly. After pretreatment, the temperature was reduced to 25 °C for the subsequent adsorption experiment. In the adsorptive desulfurization and denitrogenation, the model fuel was sent into the adsorbent column by a HPLC pump, flowed up through the adsorbent bed at a liquid hourly space velocity (LHSV) of 4.8 h^{-1}. The effluent from the top of the column was collected periodically for analysis.

Table 2
Physical properties of adsorbents

	Surface area (m^2/g)	Pore size (Å)	Particle size (μm)
Activated alumina	155	58	106
Activated carbon	1843	28.6	~150
Ni/SiO_2-Al_2O_3	157	–	150–250

The treated-fuel samples were analyzed by a SRI gas chromatograph equipped with a capillary column (XTI-5, Restek) and a flame ionized detector (FID) for quantification, using *n*-tetradecane as an internal standard. The total sulfur and nitrogen concentrations in the samples were also analyzed using Antek 9000 total sulfur/nitrogen analyzer. The detailed analysis method was mentioned in our previous paper [23].

Calculations of electronic properties of the sulfur compounds, nitrogen compounds and aromatics examined in the present study were conducted by using a semi-empirical quantum chemistry method, MOPAC-PM3, in CAChe (Version 6.1.1). The PM3 method determines both the optimum geometry and electronic properties of molecules by solving the Schrödinger equation using the PM3 semi-empirical Hamiltonians developed by Stewart [40,41]. The electrostatic potential on electron density for various adsorbates was calculated on the PM3 geometries. The computational method was described in detail in the previous papers [42,43].

3. Results

3.1. Adsorption on Ni/SiO_2-Al_2O_3

The breakthrough curves of the six species, Nap, 1-MNap, 4,6-DMDBT, DBT, quinoline and indole, over Ni/SiO_2-Al_2O_3 at 25 °C and 4.8 h^{-1} LHSV are shown in Fig. 1. The first two breakthrough compounds were Nap and 1-MNap, with almost the same breakthrough amount of the treated fuel, 1.6 g of the treated fuel per gram of adsorbent (g-F/g-A). After breakthrough, the C/C_o value (a ratio of the outlet concentration to the initial concentration in the model fuel) for the two aromatics increased sharply to over 1.0. The third breakthrough compound was 4,6-DMDBT with the breakthrough amount of 3.2 g-F/g-A. Interestingly, DBT broke through at an amount of the treated fuel of 4.9 g-F/g-A, the breakthrough amount of the treated fuel was about 1.6 times higher than that for 4,6-DMDBT. The amount of the treated fuel corresponding to the saturation point was 4.9 and 8.7 g-F/g-A, respectively, for 4,6-DMDBT and DBT. After saturation point, the C/C_o value for 4,6-DMDBT rose sharply until $C/C_o = 1.4$, while the C/C_o

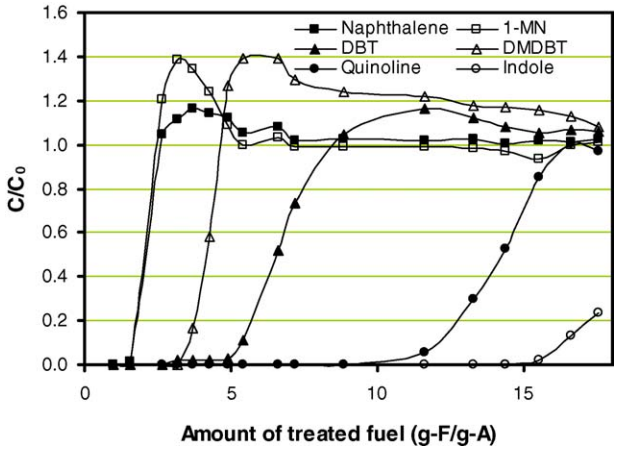

Fig. 1. Breakthrough curves of aromatic, sulfur and nitrogen compounds over Ni/SiO_2-Al_2O_3.

value for DBT increased gradually to 1.17. Quinoline and indole broke through at a treated-fuel amount of 10.0 and 15.5 g-F/g-A, respectively. According to the breakthrough order, the adsorptive selectivity for the six adsorbates increases in the order of Nap ≈ 1-MNap < 4,6-DMDBT < DBT < quinoline < indole. The breakthrough, saturation and net capacities for each species were calculated and listed in Table 3.

In order to facilitate the quantitative discussion of the adsorptive selectivity, a relative selectivity factor was used in the present study, which is defined as:

$$\alpha_{i-n} = \frac{Cap_i}{Cap_n} \quad (1)$$

where Cap_i is the adsorptive capacity of compound 'i' corresponding to the breakthrough point and Cap_n is the adsorptive capacity of the reference compound, Nap, corresponding to its breakthrough point. It should be mentioned that as using the kinetics breakthrough capacities instead of the equilibrium capacity in Eq. (1), the defined selectivity factor is not for the equilibrium selectivity. The calculated relative selectivity factor on the basis of the breakthrough curves are shown in Table 4. The α_{i-n} value is 1.0, 1.0, 2.0, 3.1, 6.6 and 10.1, respectively, for Nap, 1-MNap, 4,6-DMDBT, DBT, quinoline and indole.

Table 3
Adsorption capacities (mmol/g) of three adsorbents for each compound on the basis of GC-FID analysis

	Nap	1-MNap	DBT	DMDBT	Indole	Quinoline
Ni/SiO_2-Al_2O_3						
Breakthrough	0.017	0.017	0.052	0.039	0.167	0.125
Saturation	0.022	0.021	0.070	0.043	0.186	
Net[a]	0.015	0.016	0.061	0.013	0.186	0.151
Activated alumina						
Breakthrough	0.015	0.015	0.032	0.033	0.195	0.251
Saturation	0.019	0.020	0.040	0.038	0.227	0.289
Net	0.011	0.011	0.016	0.011	0.221	0.288
Activated carbon						
Breakthrough	0.066	0.089	0.202	0.295	0.705	0.536
Saturation	0.091	0.105	0.252	0.336	0.732	0.579
Net	0.054	0.066	0.185	0.282	0.732	0.580

[a] Net adsorptive capacity when the adsorption test was ended.

Table 4
Selectivity factor (α_{i-n}) relative to naphthalene for each compound

Selectivity[a]	Nap	1-MNap	DBT	DMDBT	Indole	Quinoline
Ni/SiO_2-Al_2O_3	1.0	1.0	3.1	2.0	10.1	6.6
Activated alumina	1.0	1.0	2.2	2.2	12.8	16.5
Activated carbon	1.0	1.3	3.0	4.5	10.6	8.1

[a] Using the relative selectivity factor as defined by Eq. (1).

3.2. Adsorption on activated alumina

The breakthrough curves of the six species over the activated alumina at 25 °C and 4.8 h^{-1} LHSV are shown in Fig. 2. Both Nap and 1-MNap broke through at a treated-fuel amount of 1.4 g-F/g-A. After the breakthrough point, the C/C_o value for the two aromatics rose sharply to about 1.4, and then, returned to 1.0 when the adsorbent was saturated by DBT and 4,6-DMDBT. 4,6-DMDBT and DBT broke through with almost the same breakthrough amount of the treated fuel (3.1 g-F/g-A). After the breakthrough, the C/C_o value for both increased synchronously to around 1.15, and then, stayed at this value until indole broke through. The C/C_o values for the two sulfur compounds decreased gradually to 1.00 while the C/C_o value for indole increased from 0 to 1.00. Indole broke through at an amount of the treated fuel of 18.9 g-F/g-A. After the breakthrough, the C/C_o value for indole increased to 1.17, and then, returned to 1.00 when the adsorbent was saturated by quinoline. The last breakthrough compounds was quinoline with the breakthrough amount of 23.2 g-F/g-A, and the treated-fuel amount corresponding to saturation point was 31.1 g-F/g-A.

The breakthrough and saturation capacities for each compound were calculated and listed in Table 3. The selectivity for each compound is listed in Table 4. The adsorptive selectivity

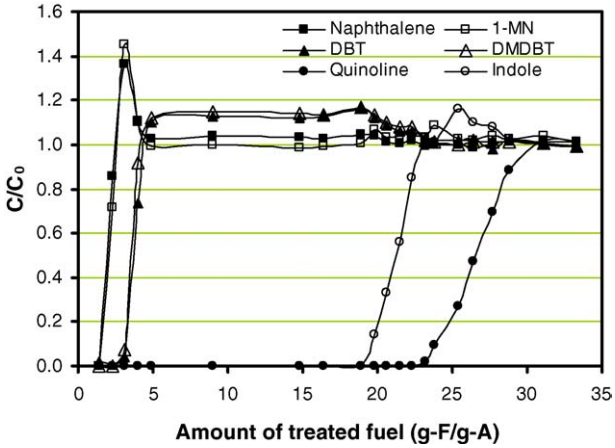

Fig. 2. Breakthrough curves of aromatic, sulfur and nitrogen compounds over the activated alumina.

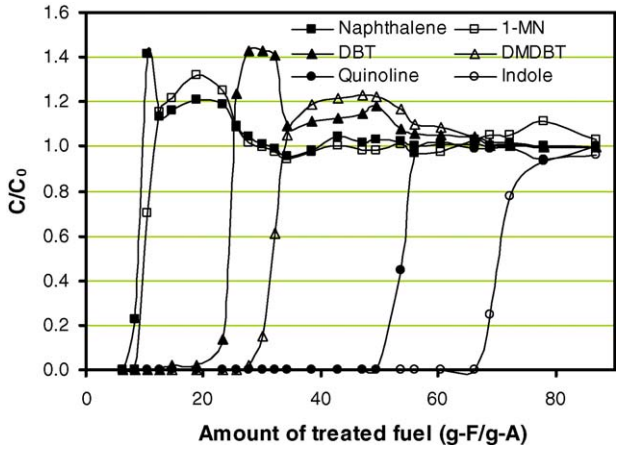

Fig. 3. Breakthrough curves of aromatic, sulfur and nitrogen compounds over the activated carbon.

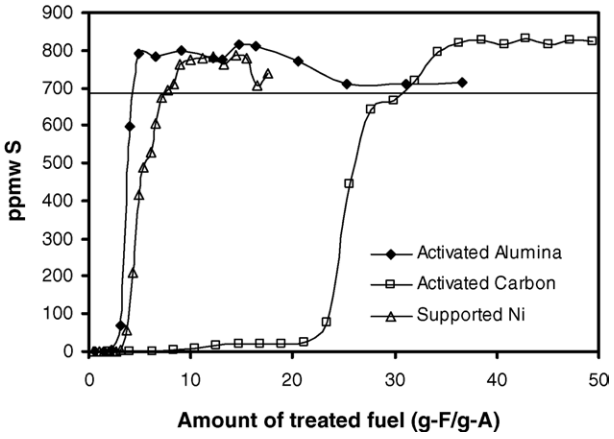

Fig. 4. Breakthrough curves for total sulfur over the three different adsorbents.

for the six compounds over the activated alumina increased in the order of Nap ≈ 1-MNap < 4,6-DMDBT ≈ DBT ≪ indole < quinoline. The relative selectivity factor (α_{i-n}) was 1.0, 1.0, 2.2, 2.2, 12.8 and 16.5, respectively, for Nap, 1-MNap, 4,6-DMDBT, DBT, indole and quinoline.

3.3. Adsorption on activated carbon

The breakthrough curves over the activated carbon at 25 °C and 4.8 h^{-1} LHSV are shown in Fig. 3. Nap broke through at a treated-fuel amount of 6.2 g-F/g-A. After the breakthrough, the C/C_o value rose sharply to over 1.4, and then, returned to 1.0 gradually at the treated-fuel amount of 30 g-F/g-A. 1-MNap broke through at a treated-fuel amount of 8.4 g-F/g-A, and then, the C/C_o value increased sharply to over 1.3. The breakthrough amount of the treated fuel for DBT was 12 g-F/g-A. After that the C/C_o values for DBT increased sharply to around 1.4, and then, stayed at this value until 4,6-DMDBT broke through. 4,6-DMDBT broke through at a treated-fuel amount of 27.6 g-F/g-A, and then, increased sharply to over 1.2. The C/C_o value for the two sulfur compounds decreased to around 1.0 when the column was saturated by quinoline. The breakthrough amount of the treated fuel for quinoline and indole was 49.3 and 66.1 g-F/g-A, respectively, and the saturation amount of the treated fuel was 60.3 and 86.7 g-F/g-A, respectively. The corresponding breakthrough and saturation capacities for each compound are listed in Table 3. The adsorptive selectivity for the six compounds over the activated carbon increased in the order of Nap < 1-MNap < 4,6-DMDBT < DBT < quinoline < indole. The relative selectivity factor (α_{i-n}) was 1.0, 1.3, 3.0, 4.5, 8.1 and 10.6, respectively, for Nap, 1-MNap, DBT, 4,6-DMDBT, quinoline and indole, as shown in Table 4.

3.4. Adsorptive capacity for total sulfur and total nitrogen over different adsorbents

The breakthrough curves for total sulfur over the three different adsorbents at 25 °C and 4.8 h^{-1} LHSV are shown in Fig. 4, where the total sulfur concentration was measured by using Antek 9000 series total sulfur/nitrogen analyzer. The breakthrough amount of the treated fuel was 2.3, 3.2 and 10.4 g-F/g-A, respectively, for the activated alumina, Ni/SiO_2-Al_2O_3 and the activated carbon, corresponding to the breakthrough capacity of 0.049, 0.068 and 0.223 mmol of sulfur per gram of adsorbent (mmol-S/g-A) or 1.57, 2.18 and 7.15 mg of sulfur per gram of adsorbent (mg-S/g-A), as shown in Table 5. The adsorbent was saturated by the sulfur when the amount of the treated fuel reached 4.9, 7.7 and 32.1 g-F/g-A, respectively, for the activated alumina, Ni/SiO_2-Al_2O_3 and the activated carbon, with the saturation adsorptive capacity of 0.075, 0.106 and 0.508 mmol-S/g-A (or 2.41, 3.40 and 16.29 mg-S/g-A), respectively. From a comparison of the three adsorbents, it is clear that the activated carbon showed much higher adsorptive capacity than Ni/SiO_2-Al_2O_3 and the activated alumina at 25 °C.

The breakthrough curves for total nitrogen over the three different adsorbents at 25 °C and 4.8 h^{-1} LHSV are shown in Fig. 5. The breakthrough amount of the treated fuel was 11.1, 19.8 and 49.3 g-F/g-A, respectively, for Ni/SiO-Al_2O_3, the activated alumina and the activated carbon, with the breakthrough capacity of 0.240, 0.427 and 1.067 mmol-N/g-A or 3.36, 5.98 and 14.94 mg-N/g-A. The saturation adsorption capacity was 0.335, 0.511 and 1.311 mmol-N/g-A (or 4.69, 7.16 and 18.37 mg-N/g-A), respectively. The adsorptive capacity for total nitrogen increased significantly in the order of Ni/SiO_2-Al_2O_3 < the activated alumina < the activated carbon.

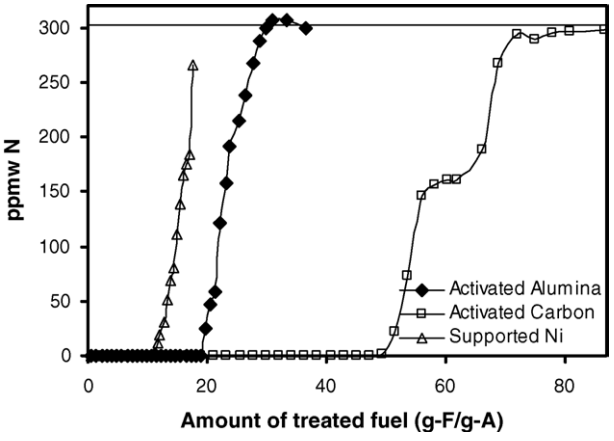

Fig. 5. Breakthrough curves for total nitrogen over the three different adsorbents.

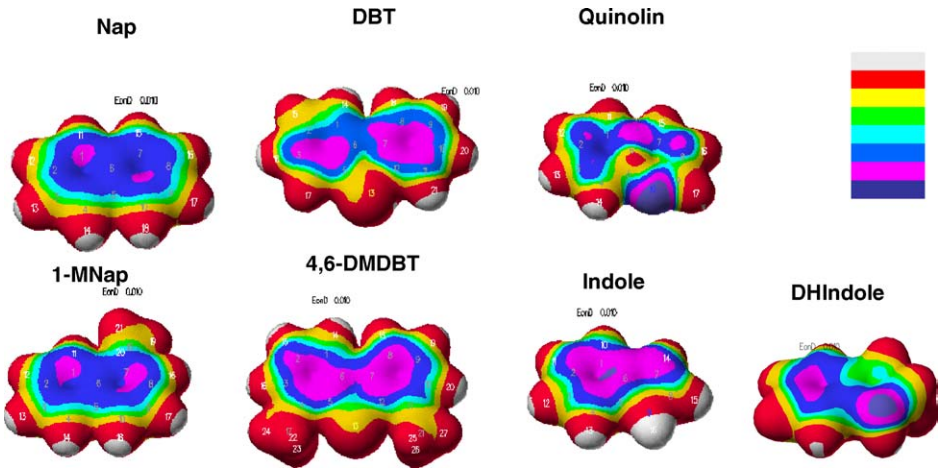

Fig. 6. Electrostatic potential on electron density for the examined compounds.

The three adsorbents showed much higher adsorption capacity for the nitrogen compounds than for the sulfur compounds.

3.5. Electronic properties of the compounds

Some electronic properties, including dipole, bond order, atomic partial charge and ionization potential, of the compounds examined in this work were calculated and the results are shown in Table 6. Dipole of the molecules increases in the order of Nap < 1-MNap < 4,6-DMDBT < DBT < quinoline < indole. The highest bond order in the molecules increases in the order of 4,6-DMDBT ≈ DBT < 1-MNap ≈ Nap < indole < quinoline. The ionization potential increases in the order of indole < 4,6-DMDBT ≈ DBT < 1-MNap < Nap < quinoline. The number of C(sp^2) atoms plus S/N atom in the molecules increases in the order of indole < quinoline = 1-MNap = Nap < DMDBT = DBT.

The electrostatic potential color-mapped on the electron density with values at the color boundaries for the seven molecules was calculated and the results are shown in Fig. 6. It shows clearly that the negative electrostatic potential are dominantly located on the two sides of the molecular plane (except quinoline), and the value of the negative electrostatic potential increases in the order of Nap < 1-MNap < DBT < 4,6-DMDBT < indole < dihydroindole. Evidently, the methyl group at the aromatic ring enhances the negative electrostatic potential on the two sides of the molecular plane because the methyl group is an electron donor to the aromatic ring. Quinoline has the highest value of the negative electrostatic potential in all examined adsorbates, but such negative domain is located on the nitrogen atom instead of the two sides of the molecular plane.

4. Discussion

4.1. Comparison of adsorptive capacity and selectivity of the three adsorbents

Adsorption performance of adsorbents usually depends on both surface chemical property, such as active sites and their density, and physical property, including surface area, pore size and distribution. The present study shows that the adsorptive capacities (both breakthrough capacity and saturation capacity) based on the adsorbent weight increase in the order of activated alumina < Ni/SiO_2-Al_2O_3 < activated carbon for total sulfur, and in the order of Ni/SiO_2-Al_2O_3 < activated alumina < acti-activated carbon for total nitrogen, indicating that the activated carbon is the best adsorbent in the three adsorbents for both total sulfur removal and total nitrogen removal. For removing total sulfur, the breakthrough capacity of the activated carbon is about 3.3 times higher than that of Ni/SiO_2-Al_2O_3 and about 4.6 times higher than that of the activated alumina. For removing nitrogen, the breakthrough capacity of the activated carbon is about 4.4 times higher than that of Ni/SiO_2-Al_2O_3 and about 2.5 times higher than that of activated alumina. It should be pointed out that nickel-based adsorbents usually have much higher capacity for removing sulfur at high temperature, such as 200 °C, as reported in our previous study [15]. However, in comparison of the adsorptive capacity based on the surface area, as shown in Table 5, it is found that Ni/SiO_2-Al_2O_3 and the activated alumina have much higher adsorptive capacity per square meter than the activated carbon for both total sulfur and total nitrogen. It implies that in the view of the surface chemical property, Ni/SiO_2-Al_2O_3 and the activated alumina are the better adsorbents than the activated carbon. The higher weight-based adsorptive capacity of the activated carbon is because the activated carbon has about 12 times higher surface area than Ni/SiO_2-Al_2O_3 and the activated alumina.

In comparison of adsorptive selectivity of the three adsorbents for the nitrogen compounds, as shown in Table 4, it is noted that Ni/SiO_2-Al_2O_3 (α_{i-n} = 10.1 and 6.6, respectively, for indole and quinoline) and the activated carbon (α_{i-n} = 10.6 and 8.1, respectively, for indole and quinoline) show the similar adsorptive selectivity, while the activated alumina has significantly higher adsorptive selectivity (α_{i-n} = 12.8 and 16.5, respectively, for indole and quinoline) than both Ni/SiO_2-Al_2O_3 and the activated carbon. For the sulfur compounds, Ni/SiO_2-Al_2O_3 and the activated carbon show the similar adsorptive selectivity for DBT (α_{i-n} = 3.0–3.1), while the activated alumina has lower adsorptive selectivity for DBT (α_{i-n} = 2.2). Interestingly, the activated

Table 5
Adsorption capacities for total sulfur and total nitrogen on the basis of the total sulfur/nitrogen analysis

	Based on weight				Based on surface area	
	Total S		Total N		Total S (μmol/m^2)	Total N (μmol/m^2)
	mmol/g	mg-S/g	mmol/g	mg-N/g		
Ni/SiO_2-Al_2O_3						
Breakthrough	0.068	2.18	0.240	3.36	0.433	1.529
Saturation	0.106	3.40	0.335	4.69	0.675	2.134
Activated alumina						
Breakthrough	0.049	1.57	0.427	5.98	0.316	2.755
Saturation	0.075	2.41	0.511	7.16	0.484	3.297
Activated carbon						
Breakthrough	0.223	7.15	1.067	14.94	0.121	0.579
Saturation	0.508	16.29	1.311	18.37	0.276	0.711

carbon shows about two times higher adsorptive selectivity for 4,6-DMDBT ($\alpha_{i-n} = 4.5$) than both Ni/SiO_2-Al_2O_3 and the activated alumina. Consequently, in terms of both adsorptive capacity and selectivity for 4,6-DMDBT, the activated carbon should be the best adsorbent among the three adsorbents for adsorptive desulfurization of the commercial diesel fuel and low-sulfur diesel fuel, as the major sulfur compounds existing in these fuels are the alkyl DBTs with two alkyl groups at the 4- and 6-positions of DBTs.

4.2. Adsorption mechanism over different adsorbents

The results in the present study show that the adsorptive selectivity of the three different adsorbents for various compounds is quite different. It implies that adsorption of the sulfur and nitrogen compounds on different adsorbents might obey different adsorption mechanisms. Combination of the observed adsorptive selectivity and electronic properties of the different compounds might provide a close insight into the fundamental understanding of the adsorption mechanisms.

4.2.1. Adsorption on Ni/SiO_2-Al_2O_3

For adsorption on Ni/SiO_2-Al_2O_3, the adsorptive selectivity increases in the order of Nap ($\alpha_{i-n} = 1.0$) $\approx$ 1-MNap ($\alpha_{i-n} = 1.0$) < 4,6-DMDBT ($\alpha_{i-n} = 2.0$) < DBT ($\alpha_{i-n} = 3.1$) < quinoline ($\alpha_{i-n} = 6.6$) < indole ($\alpha_{i-n} = 10.1$), as shown in Fig. 1 and Table 4. No direct relationship between this order and the calculated molecular properties, including ionization, net atomic charge on S or N, the highest bond order, or dipole magnitude, was observed, indicating the adsorption mechanism cannot be simply explained by these molecular properties. However, this selectivity order indicates clearly that methyl groups on the 4- and 6-position of DBT strongly inhibit the adsorption of 4,6-DMDBT on Ni/SiO_2-Al_2O_3, while the methyl group on naphthalene shows almost no effect on adsorption of naphthalenes on Ni/SiO_2-Al_2O_3. Since the two methyl groups in 4,6-DMDBT are adjacent to the sulfur atom, as shown in Fig. 6, it is reasonable to infer that a direct interaction between the sulfur atom and the surface nickel on Ni/SiO_2-Al_2O_3 might play an important role in the selective adsorption of sulfur compounds and the two methyl groups at the 4- and 6-positions block the approach of the sulfur atom to the surface nickel atom. The observed results support further the adsorption mechanism involving a direct coordination between the sulfur atom and the surface nickel, which was proposed in our previous study [24].

On the other hand, as well known, quinoline is a basic nitrogen compound and indole is a neutral nitrogen compound. Ni/SiO_2-Al_2O_3 selectively adsorbs indole over quinoline, indicating that the acid–base interaction does not play an important role in the adsorption over Ni/SiO_2-Al_2O_3. Hydrogenation of indole probably occurs on the nickel surface, as there are probably some active hydrogen atoms on the nickel surface, like the hydrogenation of benzothiophene and 1-octene on the nickel surface observed in the previous study [24]. This hydrogenation results in formation of dihydroindole, which has much higher negative electrostatic potential (see Fig. 6) and lower net atomic charge (see Table 6) on the nitrogen atom than that in indole. This is probably why Ni/SiO_2-Al_2O_3 shows higher selectivity for indole.

Another interesting phenomenon found in the present study is that after passing through the saturation point ($C/C_o = 1$), the outlet concentration of some compounds, especially the aromatics and DBTs, increases continuously over its initial concentration in the model fuel by even more than 40% ($C/C_o > 1.4$). After passing the maximum value, the outlet concentration decreases gradually to the initial one, while the concentration of the following breakthrough compound increases to $C/C_o = 1$. It can be inferred from this phenomenon that: (1) the adsorption of such compounds is at least partially reversible; (2) the compounds have relatively lower adsorptive affinity than the subsequently breakthrough compounds, resulting in at least partly replacement of the compounds with lower adsorptive affinity by the compounds with higher adsorptive affinity. As shown in Fig. 1, the area between the breakthrough curve of the compound and line $C_t/C_o = 1$ before the saturation point represents the amount of the adsorbed molecules, while the area between the breakthrough curve and line $C_t/C_o = 1$ after the saturation point represents the amount of the replaced molecules. Comparison of these two areas

Table 6
The calculated properties of adsorbates

Adsorbate	Ionization (eV)	Charge on S or N[a] (a.u.)	Number of $C(sp^2)$ + S/N	The highest bond order	Dipole magnitude (D)
S compounds					
DBT	8.598	+0.243	13	1.449	1.362
4,6-DMDBT	8.511	+0.240	13	1.442	0.748
N compounds					
Quinoline	9.241	−0.060	10	1.652	1.844
Indole	8.355	+0.288	9	1.628	2.004
Dihydroindole	8.521	+0.032	7	1.446	1.320
Aromatics					
Nap	8.835		10	1.608	0.000
1-MNap	8.712		10	1.607	0.270

[a] Net atomic charge.

provides further information about the competitive adsorption of different species on the adsorbents. The net adsorptive capacities for each compound over the three adsorbents were calculated by subtracting the amount of the replaced molecules from the saturation capacity, and the results are listed in Table 3.

For the adsorption on Ni/SiO_2-Al_2O_3 as shown in Fig. 1 and Table 3, it is clear that a part of the adsorbed naphthalenes can be replaced by the sulfur compounds. About 70% of the adsorbed 4,6-DMDBT molecules can be replaced by DBT, indicating that this part of adsorption of 4,6-DMDBT molecules is reversible and the adsorptive affinity of DBT over Ni/SiO_2-Al_2O_3 is higher than that of 4,6-DMDBT probably due to the steric hindrance of the methyl groups in 4,6-DMDBT. It is also found in Fig. 1 that the majority of the adsorbed DBT molecules (>87%) cannot be replaced by the nitrogen compounds, indicating that DBT adsorption on Ni/SiO_2-Al_2O_3 is too strong to be replaced by the nitrogen compounds or at least a part of DBT adsorption is even irreversible. This is consonant with our foregoing discussion that considerable part of thiophenic molecules are adsorbed on the nickel-based adsorbent through the direct coordination between the sulfur atom and the nickel instead of the π-electrons on the aromatic ring. This interaction probably can result in the formation of surface nickel sulfides [24].

In summary, there are probably two adsorption configurations of the thiophenic sulfur compounds over the nickel-based adsorbent, the end-on adsorption and the side-on adsorption. In the end-on adsorption configuration, the sulfur atom in the thiophenic compounds interacts directly with the surface nickel atom, probably through η^1S and/or S-μ3 coordination geometries [3]. In this case, evidently, alkyl substituents adjacent to the sulfur atom inhibit the adsorption of the sulfur compounds on the adsorption sites, as observed for 4,6-DMDBT adsorption. In the side-on adsorption configuration, the sulfur compounds are adsorbed flat on the adsorption site, in which π-electrons on the aromatic rings might play an important role.

4.2.2. Adsorption on the activated alumina

For adsorption on the activated alumina, the adsorptive selectivity for the various species increases in the order of Nap ≈ 1-MNap < 4,6-DMDBT ≈ DBT < indole < quinoline. This selectivity pattern does not match with the calculated molecular properties listed in Table 6, but is similar to their negative electrostatic potential, as shown in Fig. 6. It suggests that the electrostatic effect might play an important role in the adsorption of such compounds on the activated alumina. The results also suggest that the adsorption occurs likely through a side-on adsorption configuration. On the other hand, the activated alumina used in this study is an acidic activated alumina, while quinoline is a basic compound and indole is a non-basic compound. The higher adsorptive selectivity of the activated alumina for quinoline than that for indole can be attributed to the acid–base interaction. Consequently, the acid–base interaction might also play an important role in determining the adsorptive selectivity of the activated alumina. This acid–base interaction occurs probably through an end-on adsorption configuration. It should be pointed out that the methyl groups on the aromatic ring in naphthalene and DBT appear to have almost no effect on their adsorptive selectivity over the activated alumina, although the methyl groups increase the negative electrostatic potential on the aromatic rings.

As shown in Fig. 2 and Table 3, nearly a half of the adsorbed aromatics can be replaced (displaced) by the sulfur compounds, and the majority of the adsorbed sulfur compounds can be replaced by indole, indicating that these compounds compete probably for the same adsorption sites, and indole has higher adsorptive affinity than the naphthalenes and DBTs. Interestingly, only very few of the adsorbed indole can be replaced by quinoline, implying that the quinoline might also be adsorbed on the sites different from the sites for indole. This is in agreement with the foregoing discussion that the adsorption of quinoline on the activated alumina might also be through an acid–base interaction. For quinoline, no above-the-feed-concentration phenomenon at outlet was observed because no compound in the present model fuel can replace the adsorbed quinoline.

4.2.3. Adsorption on the activated carbon

For adsorption on the activated carbon, the adsorptive selectivity for the various species increases in the order of Nap (α_{i-n} = 1.0) < 1-MNap (α_{i-n} = 1.3) < DBT (α_{i-n} = 3.0) < 4,

6-DMDBT ($\alpha_{i-n} = 4.5$) < quinoline ($\alpha_{i-n} = 8.1$) < indole ($\alpha_{i-n} = 10.6$). There appears to be no direct relationship between this order and the calculated molecular properties listed in Table 6, indicating the adsorption mechanism cannot be simply explained by these molecular properties. Unlike on Ni/SiO_2-Al_2O_3 and the activated alumina, the methyl groups on the aromatic rings show a significant and positive effect on the adsorptive selectivity. As is well known, the methyl substituent is an electron donor to the aromatic rings, leading to increase of π-electron density on the aromatic rings. The increase in the negative electrostatic potential on the two side of the molecular plane by the methyl substituent was confirmed by the calculation, as shown in Fig. 6.

From comparison of the adsorptive selectivity order with the negative electrostatic potential order, it is found that the order for quinoline and indole do not match with each other, indicating that the adsorptive selectivity over the activated carbon cannot be ascribed simply to the electrostatic interaction. There are many oxygen functional groups on the surface of activated carbons, which can be separated as the acidic groups, such as carboxyl and phenol groups, and basic groups, such as ketone and chromene groups. Quinoline can have a strong interaction with the acidic groups, while indole might interact with both the acidic and basic groups due to the weak acidity of the H bonded to the N atom and the weak basicity of the N atom in indole. This probably is why the activated carbon shows higher adsorptive selectivity for indole than for quinoline. Hydrogen bonding interaction might play an important role in adsorptive desulfurization and denitrogenation over the activated carbon.

Fig. 3 also indicates that 1-MNap can take over (displace) a part of the adsorbed Nap, and 4,6-DMDBT can take over (displace) a part of the adsorbed DBT, which is in agreement with their selectivity order. It indicates that the methyl groups enhance the adsorption affinity or interaction probably through increasing the electron density of the aromatic system. Indole cannot take over even a part of the adsorbed quinoline although it breaks through later than quinoline, which implies that indole probably is also adsorbed on other adsorption sides.

The presence of methyl substituents on DBT enhances the adsorptive selectivity of the activated carbon for them, suggesting that the activated carbon materials may be promising adsorbents for the adsorptive desulfurization of diesel fuel, as the major refractory sulfur compounds in the current commercial diesel fuel are methyl DBTs with methyl groups at the 4- and/or 6-positions, which are difficult to be removed by the conventional HDS process and the nickel-based adsorbents.

5. Summary

Liquid-phase adsorption of a model diesel fuel containing aromatics, sulfur and nitrogen compounds over three typical adsorbents was conducted in a fixed-bed adsorption system. Different breakthrough curves and selectivities for different compounds provided a new insight into the fundamental understanding of the adsorption mechanism over various adsorbents.

For the supported nickel adsorbent, the direct interaction between the heteroatom in the adsorbate and the surface nickel plays an important role, indicating that the supported nickel adsorbent is good for selective removal of the sulfur compounds, which have no alkyl steric hindrance, from hydrocarbon streams, such as gasoline, kerosene and jet fuel.

The adsorption selectivity of the activated alumina depends dominantly on the electrostatic interaction and the acid–base interaction. The activated alumina is very effective for selective separation of nitrogen compounds, especially for basic nitrogen compounds, but not very successful for separating the sulfur compounds from hydrocarbon streams.

The activated carbon shows higher adsorptive capacity and selectivity for both sulfur and nitrogen compounds, especially for the sulfur compounds with methyl groups, such as 4,6-DMDBT. The adsorption affinity on activated carbon cannot be simply ascribed to the negative electrostatic potential. Hydrogen bonding interaction involving surface functional groups might play an important role in adsorptive desulfurization and denitrogenation over the activated carbon. Different adsorbents may be suitable for separating different sulfur compounds from different hydrocarbon streams. Combination of two or more adsorbents in an adsorptive desulfurization process might be promising for a practical ultra-deep desulfurization process of diesel fuel.

Acknowledgements

We are pleased to acknowledge the support of this work by the US Environmental Protection Agency through NSF/EPA TSE Grant R831471. Chunshan Song wishes to thank the US Department of State, US-UK Fulbright Commission and the US Council for International Exchange of Scholars, for the Fulbright Distinguished Scholar award in conjunction with a sabbatical at the Department of Chemical Engineering, Imperial College London, University of London, UK, during 2004–2005.

References

[1] C.S. Song, An overview of new approaches to deep desulfurization for ultra-clean gasoline, diesel fuel and jet fuel, Catal. Today 86 (2003) 211–263.
[2] M. Breysse, G. Djega-Mariadassou, S. Pessayre, C. Geantet, M. Vrinat, G. Perot, M. Lemaire, Deep desulfurization: reactions, catalysts and technological challenges, Catal. Today 84 (3–4) (2003) 129–138.
[3] H. Topsoe, B.S. Clausen, F.E. Massoth, Hydrotreating Catalysis. Science and Technology, Springer-Verlag, Berlin, 1996, 310 pp.
[4] B.C. Gates, H. Topsoe, Polyhedron 16 (1997) 3213.
[5] H. Topsoe, Developments in operando studies and in situ characterization of heterogeneous catalysts, J. Catal. 216 (1–2) (2003) 155–164.
[6] Prins R, Catalytic hydrodenitrogenation, Adv. Catal. 46 (2002) 399–464.
[7] C. Song, X. Ma, New design approaches to ultra-clean diesel fuels by deep desulfurization and deep dearomatization, Appl. Catal. B. Environ. 41 (2003) 207–238.
[8] P.T. Vasudevan, J.L.G. Fierro, A review of deep hydrodesulfurization catalysis, Catal. Rev. Sci. Eng. 38 (2) (1996) 161–188.
[9] J.A. Babich, J.A. Moulijn, Science and technology of novel processes for deep desulfurization of oil refinery streams: a review, Fuel 82 (2003) 607–631.
[10] D.D. Whitehurst, T. Isoda, I. Mochida, Adv. Catal. 42 (1998) 345.

[11] S.T. Oyama, Novel catalysts for advanced hydroprocessing: transition metal phosphides, J. Catal. 216 (1–2) (2003) 343–352.
[12] X. Ma, K. Sakanishi, I. Mochida, Hydrodesulfurization reactivities of various sulfur compounds in diesel fuel, Ind. Eng. Chem. Res. 33 (1994) 218–222.
[13] T.C. Ho, Property–reactivity correlation for HDS of middle distillates, Appl. Catal. A. 244 (1) (2003) 115–128.
[14] G.C. Laredo, E. Altamirano, J.A. De los Reyes, Appl. Catal. A 243 (2003) 207–214.
[15] P. Zeuthen, K.G. Knudsen, D.D. Whitehurst, Organic nitrogen compounds in gas oil blends, their hydrotreated products and the importance to hydrotreatment, Catal. Today 65 (2–4) (2001) 307–314.
[16] S. Shin, H. Yang, K. Sakanishi, I. Mochida, D.A. Grudoski, J.H. Shinn, Appl. Catal. A 205 (2001) 101–108.
[17] Y. Sano, K.H. Choi, Y. Korai, I. Mochida, Appl. Catal. B Environ. 49 (2004) 219–225.
[18] G.W. Bailey, G.A. Swan, G.A, US Patent, 4,634,515, 1987.
[19] L.J. Bonvillr, C.L. DeGeorge, P.F. Foley, J. Garow, R.R. Lesieur, J.L.v Perston, D.F. Szydlowski, US Patent 6,159,256, 2000.
[20] R.R. Lesieur, C. Teeling, J.J. Sangiovanni, L.R. Boedeker, Z.A. Dardas, H. Huang, J. Sun, X. Tang, L.J. Spadaccini, US Patent 6,454,935, 2002.
[21] X. Ma, M. Sprague, L. Sun, C. Song, Deep desulfurization of gasoline by SARS process using adsorbent for fuel cells, Prep. Am. Chem. Soc. Div. Fuel. Chem. 47 (2002) 452–453.
[22] T. Fukunaga, H. Katsuno, H. Matsumoto, O. Takahashi, Y. Akai, Development of kerosene fuel processing system for PEFC, Catal. Today 84 (2003) 197–200.
[23] X. Ma, S. Velu, J.H. Kim, C. Song, Deep desulfurization of gasoline by selective adsorption over solid adsorbents and impact of analytical methods on ppm-level sulfur quantification for fuel cell applications, Appl. Catal. B: Environ. 56 (2005) 137–147.
[24] X. Ma, M. Sprague, C. Song, Deep desulfurization of gasoline by selective adsorption over nickel-based adsorbent for fuel cell applications, Ind. Eng. Chem. Res. 44 (2005) 5768–5775.
[25] B.S. Turk, R.P. Gupta, RTI's TReND process for deep desulfurization of naphtha, Prepr. Pap.-Am. Chem. Soc., Div. Pet. Chem. 46 (2) (2001) 392–393.
[26] S. Watanabe, X. Ma, C. Song, Selective sulfur removal from liquid hydrocarbons over regenerable CeO_2–TiO_2 adsorbents for fuel cell applications, Prepr. Pap.-Am. Chem. Soc., Div. Pet. Chem. 49 (2) (2004) 511.
[27] X. Ma, V. Velu, L. Sun, C. Song, Adsorptive desulfurization of diesel fuel over a metal sulfide-based adsorbent, Prepr. Pap.-Am. Chem. Soc., Div. Pet. Chem. 48 (2) (2003) 522–523.
[28] R.T. Yang, A.J. Hernandez-Maldonado, F.H. Yang, Desulfurization of transportation fuels with zeolites under ambient conditions, Science 301 (2003) 79–81.
[29] A.J. Hernandez-Maldonado, R.T. Yang, Desulfurization of commercial liquid fuels by selective adsorption via π-complexation with Cu(I)-Y zeolite, Ind. Eng. Chem. Res. 42 (2003) 3103–3110.
[30] A.J. Hernandez-Maldonado, R.T. Yang, New sorbents for desulfurization of diesel fuels via π-complexation, AIChE J. 50 (2004) 791–801.
[31] S. Velu, X. Ma, C. Song, Selective adsorption for removing sulfur from jet fuel over zeolite-based adsorbents, Ind. Eng. Chem. Res. 42 (2003) 5293–5304.
[32] A.J. Hernandez-Maldonado, S.D. Stamatis, R.T. Yang, A.Z. He, W. Cannella, New sorbents for desulfurization of diesel fuels via pi-complexation: layered beds and regeneration, Ind. Eng. Chem. Res. 43 (2004) 769–776.
[33] S. Haji, C. Erkey, Removal of dibenzothiophene from model diesel by adsorption on carbon aerogels for fuel cell applications, Ind. Eng. Chem. Res. 42 (2003) 6933–6937.
[34] Y. Sano, K. Choi, Y. Korai, I. Mochida, Energy Fuels 18 (2004) 644–651.
[35] Y. Sano, K. Choi, Y. Korai, I. Mochida, Appl. Catal. B Environ. 49 (2004) 219–225.
[36] A. Zhou, X. Ma, C. Song, Deep desulfurization of diesel fuels by selective adsorption with activated carbons, Prep. Pap. Am. Chem. Soc. Div. Pet. Chem. 49 (2004) 329–332.
[37] Hydrocarbon Processing, May, 1999, p. 39.
[38] R.L. Irvine, US Patent 5,730,860, 1998.
[39] S. Velu, X. Ma, C. Song, M. Namazian, S. Sethuraman, G. Venkataraman, Desulfuriation of JP-8 Jet fuel by selective adsorption over a Ni-based adsorbent for micro solid oxide fuel cells, Energy Fuels 19 (2005) 1116–1125.
[40] J.J.P. Stewart, Optimization of parameters for semiempirical methods 1, Method J. Comp. Chem. 10 (1989) 209–220.
[41] J.J.P. Stewart, Optimization of parameters for semiempirical methods 2, Appl. J. Comp. Chem. 10 (1989) 221–264.
[42] X. Ma, K. Sakanishi, T. Isoda, I. Mochida, Quantum chemical calculation on the desulfurization reactivities of heterocyclic sulfur compounds, Energy Fuels 9 (1995) 33–37.
[43] X. Ma, H.H. Schobert, Estimating heats of formation of hydrocarbon radicals by a combination of semiempirical calculation and family correlation with experimental values, J. Phys. Chem. 104 (2000) 1064–1074.